Electronic Supplementary Information for

Hierarchical Z-Scheme Fe_2O_3@$ZnIn_2S_4$ Core-Shell Heterostructures with Enhanced Adsorption Capacity Enabling Significantly Improved Photocatalytic CO_2 Reduction

By Zihan Zhao[a,#], Chuanxin Shi[a,#], Qi Shen[a,*], Wenjuan Li[b], Dandan Men[b], Bo Xu[a], Yiqiang Sun[a,*], Cuncheng Li [a,*]

More supplementary figures:

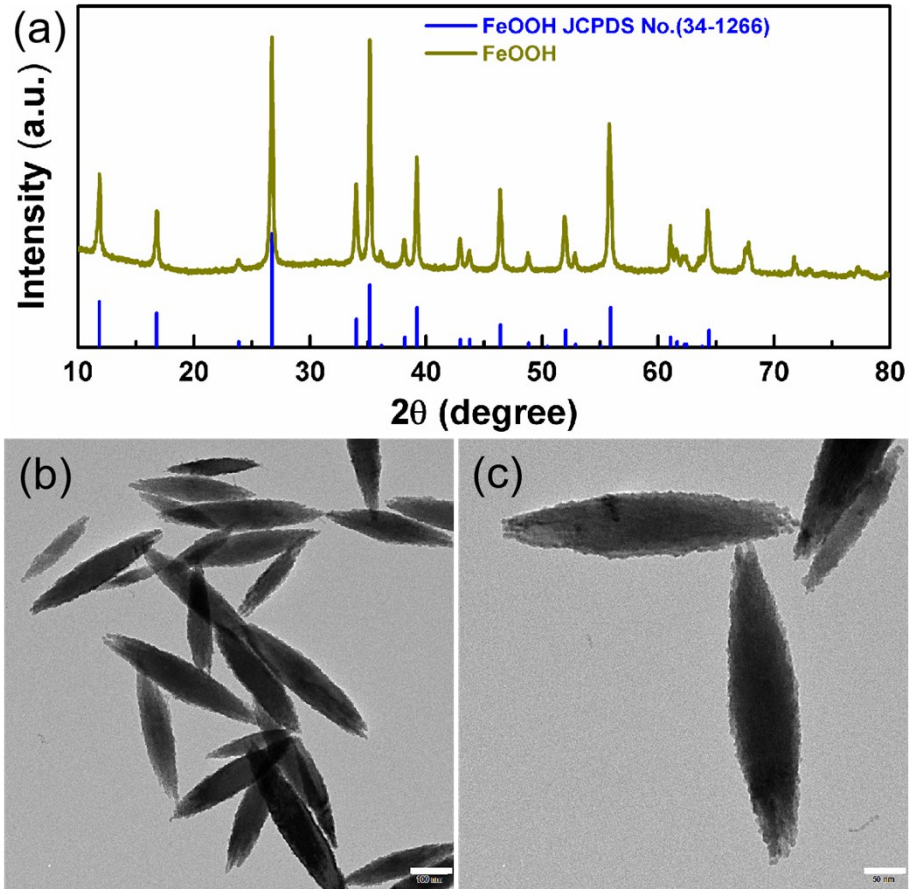

Figure S1. FeOOH nanorods precursor. (a) XRD pattern. (b) Low-magnification and (c) High-magnification TEM image.

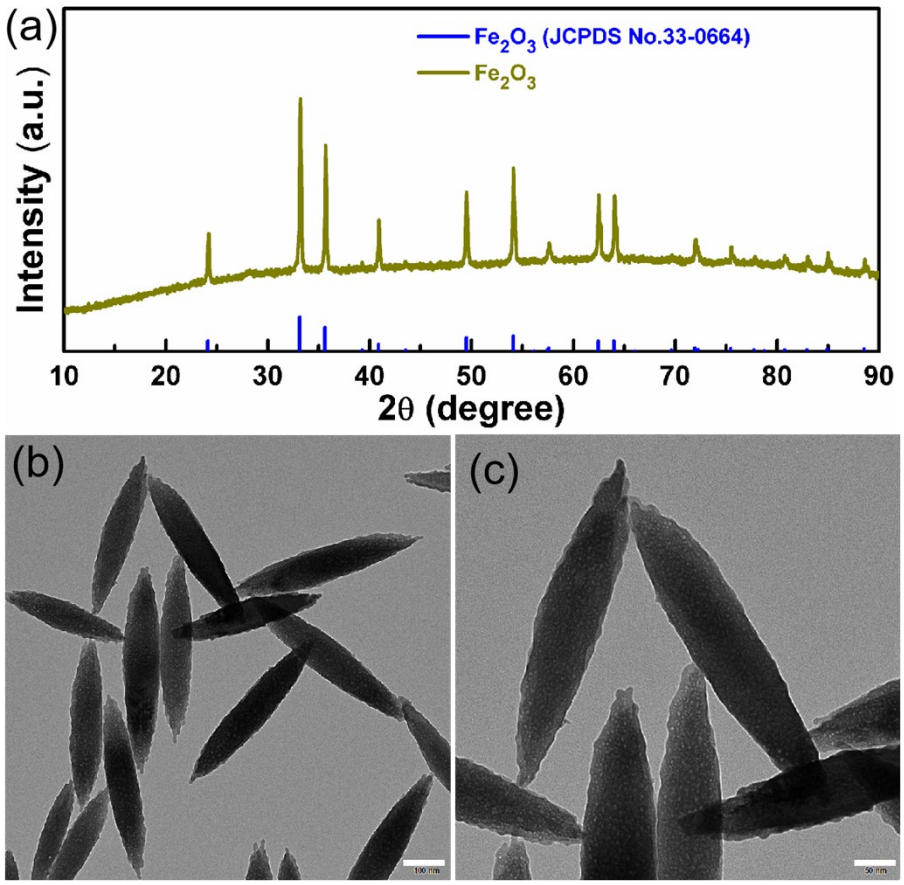

Figure S2. Fe_2O_3 nanorods. (a) XRD pattern. (b) Low-magnification and (c) High-magnification TEM image.

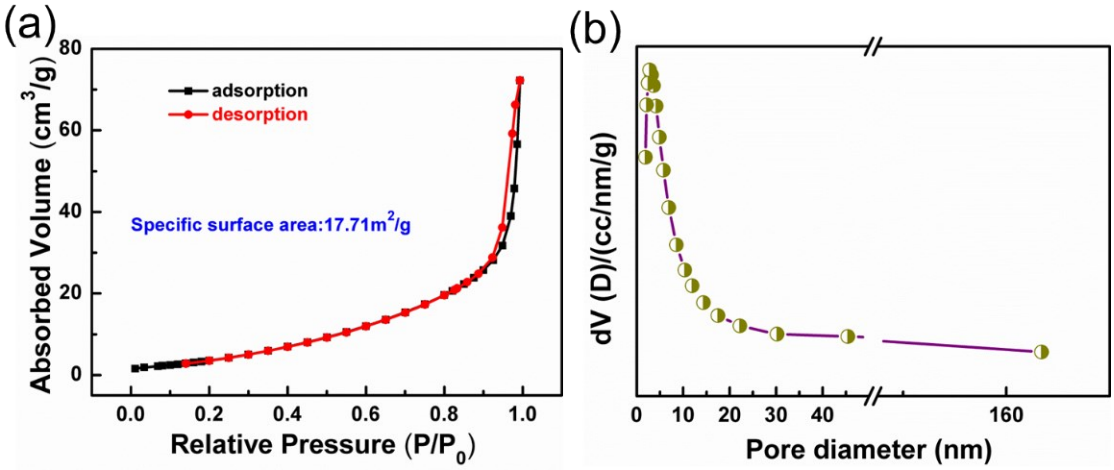

Figure S3. (a) N_2 adsorption-desorption isotherms and (b) corresponding pore size distribution for Fe_2O_3 nanorods.

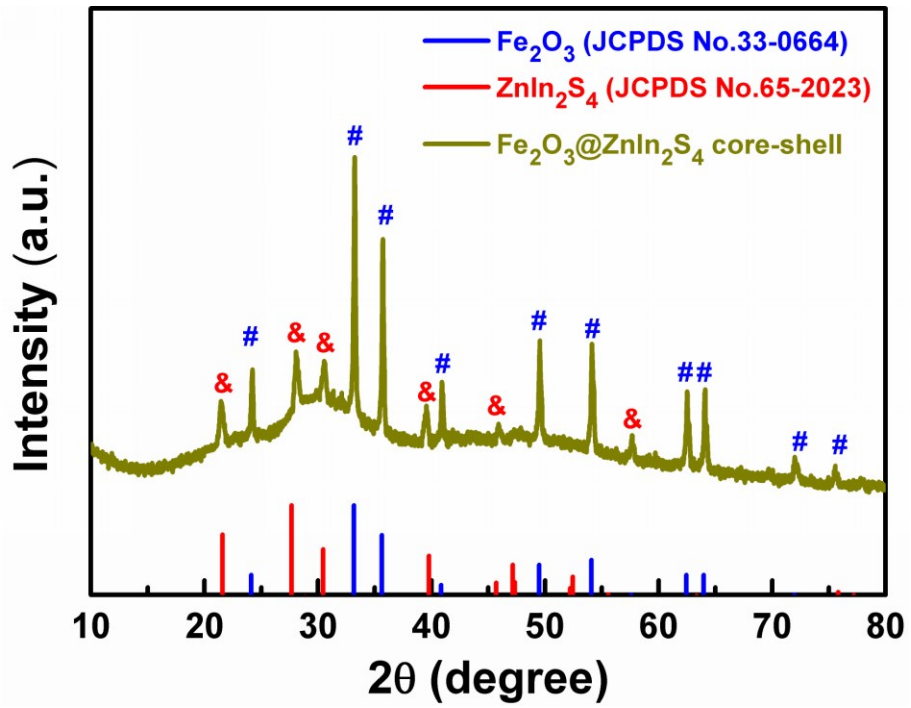

Figure S4. XRD pattern of as-prepared Fe_2O_3@$ZnIn_2S_4$ core-shell nanorods.

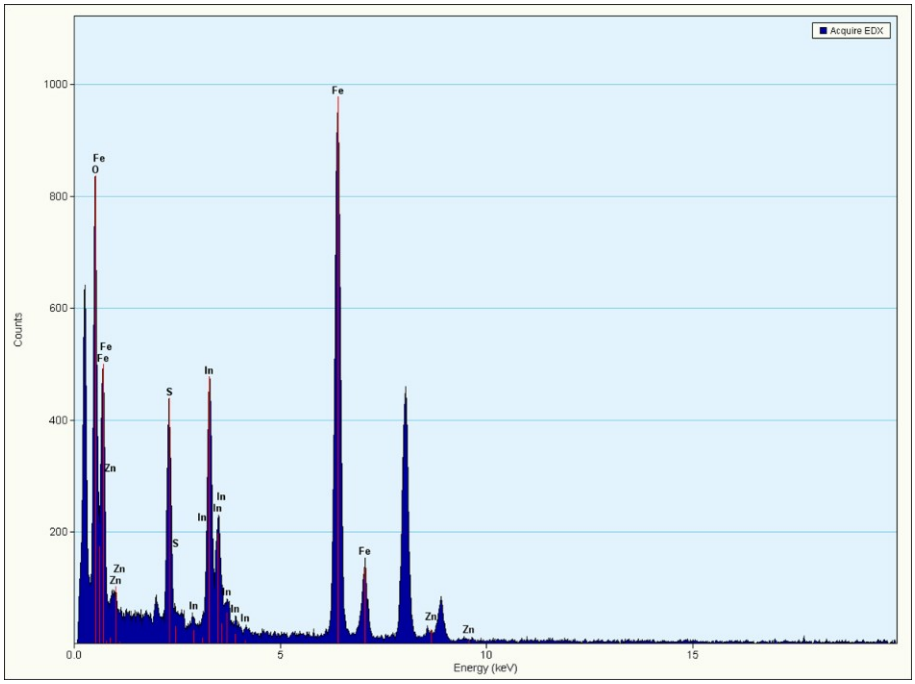

Figure S5. EDX spectrum of as-prepared Fe_2O_3@$ZnIn_2S_4$ core-shell nanorods.

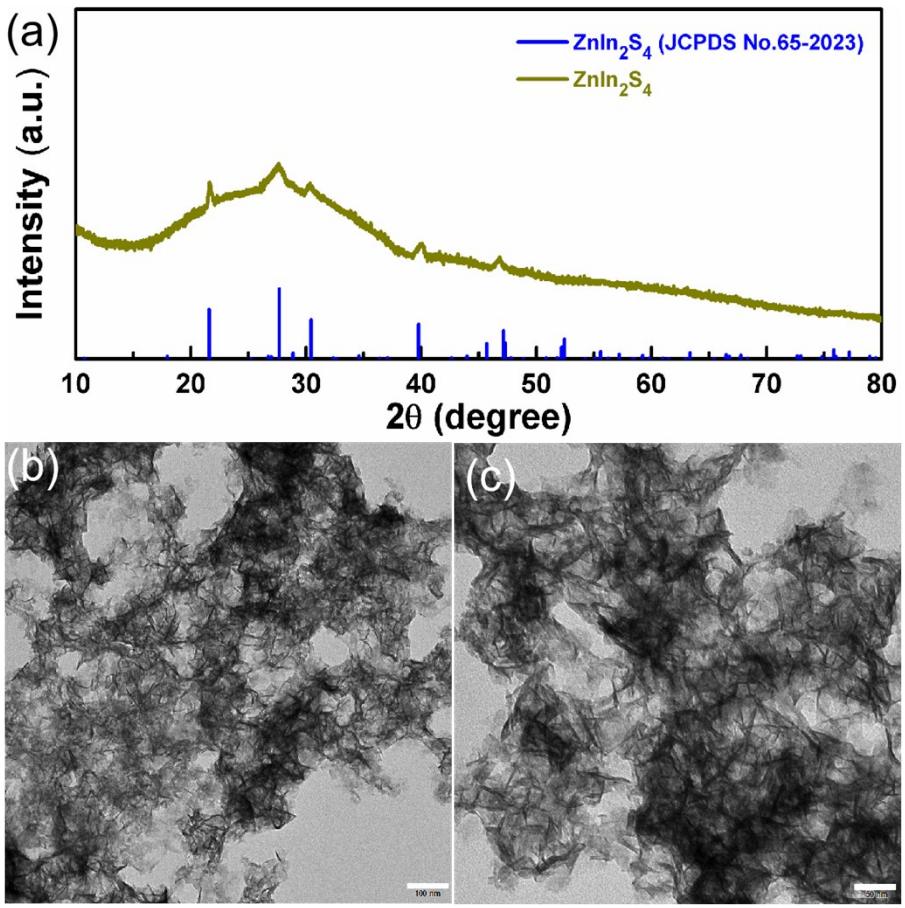

Figure S6. $ZnIn_2S_4$ nanosheets. (a) XRD pattern. (b) Low-magnification and (c) High-magnification TEM image.

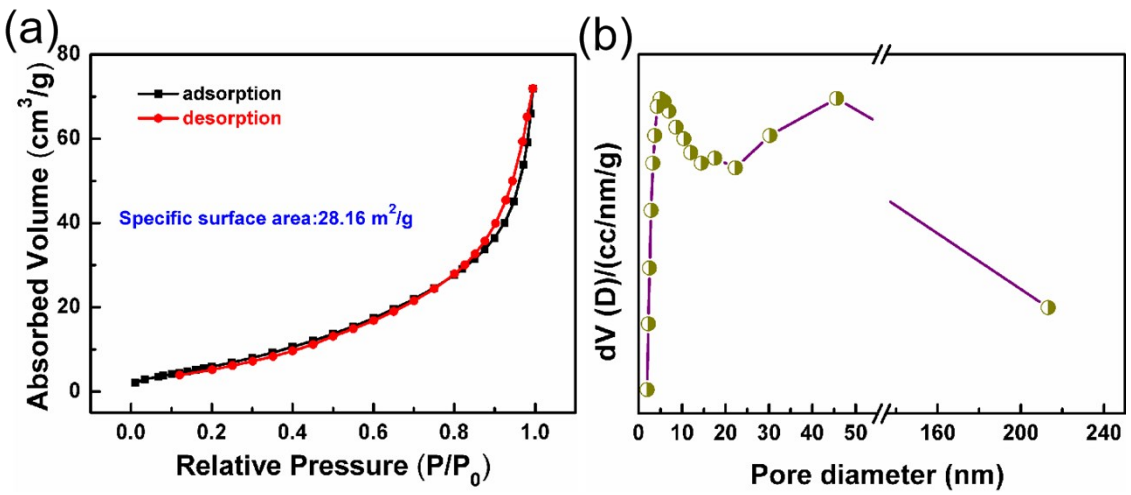

Figure S7. (a) N_2 adsorption-desorption isotherms and (b) corresponding pore size distribution for $ZnIn_2S_4$ nanosheets.

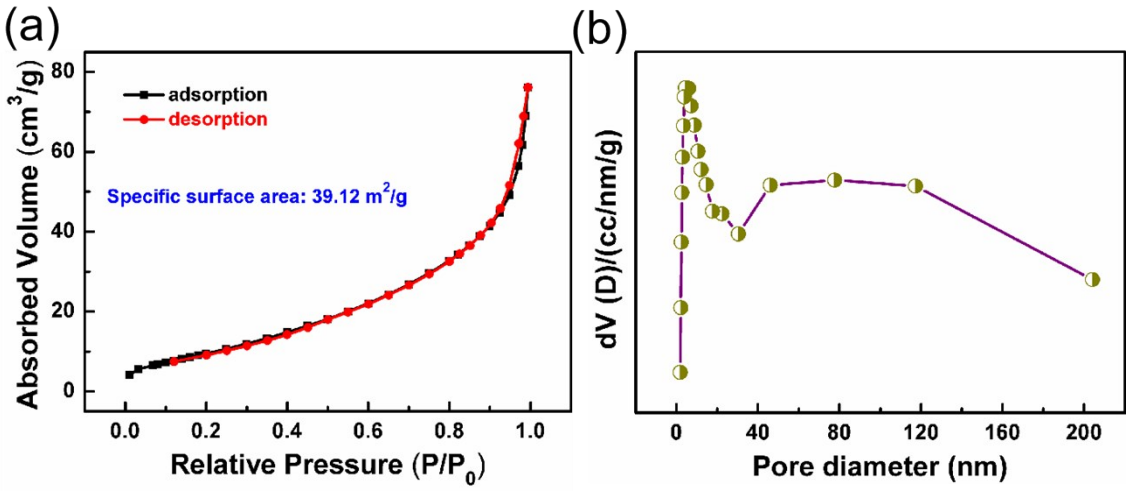

Figure S8. (a) N_2 adsorption-desorption isotherms and (b) corresponding pore size distribution for Fe_2O_3@$ZnIn_2S_4$ core-shell heterostructures.

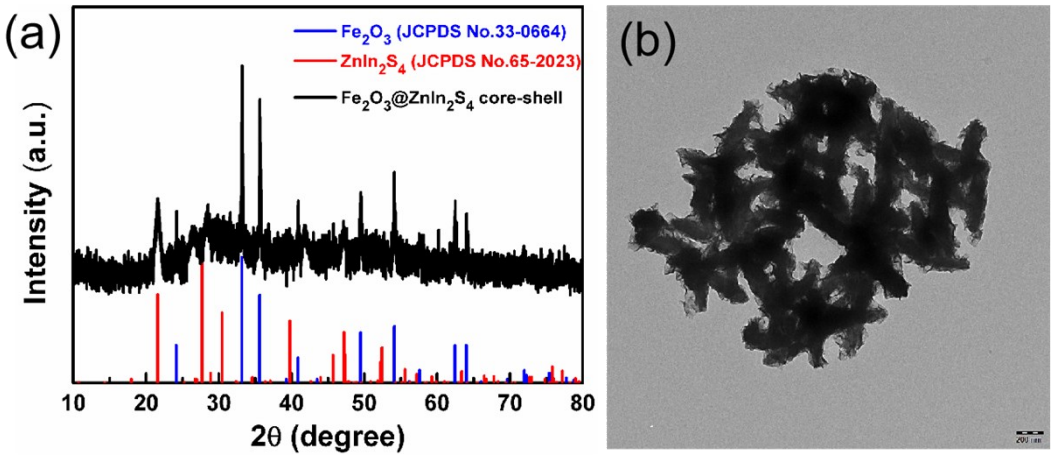

Figure S9. Fe_2O_3@$ZnIn_2S_4$ after repeated three rounds of photoreduction reaction.(a) XRD pattern and (b) TEM image.

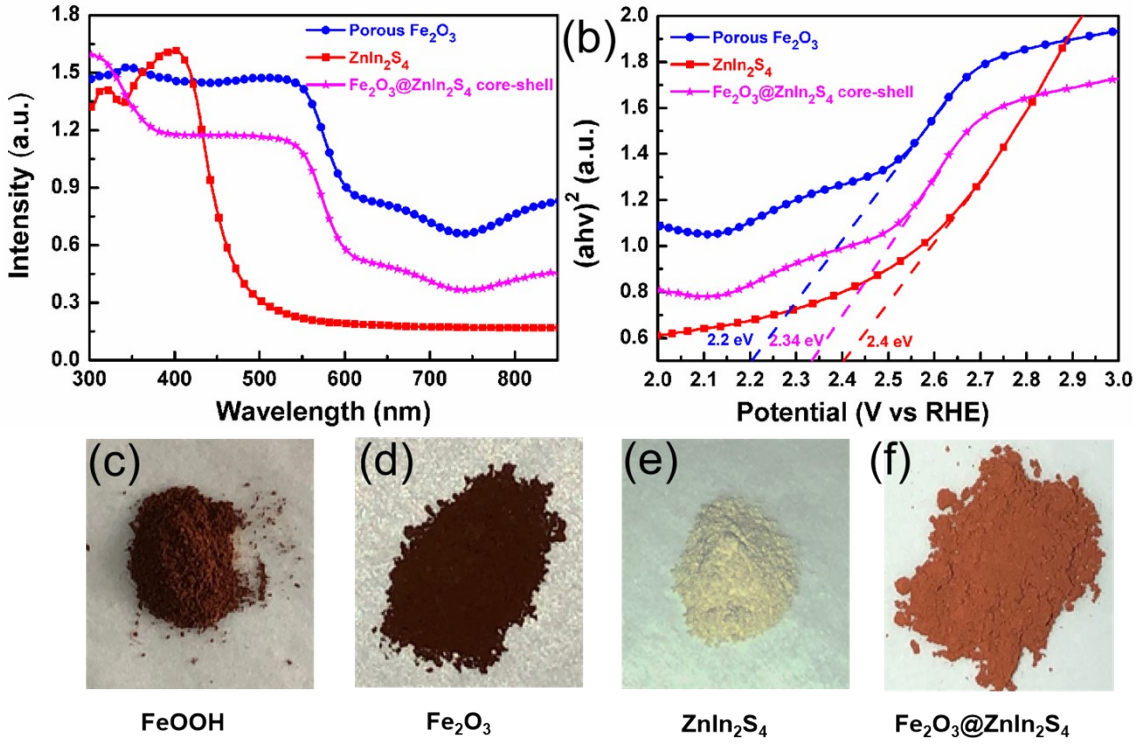

Figure S10. (a) N_2 adsorption-desorption isotherms and (b) corresponding pore size distribution for Fe_2O_3@$ZnIn_2S_4$ core-shell heterostructures.

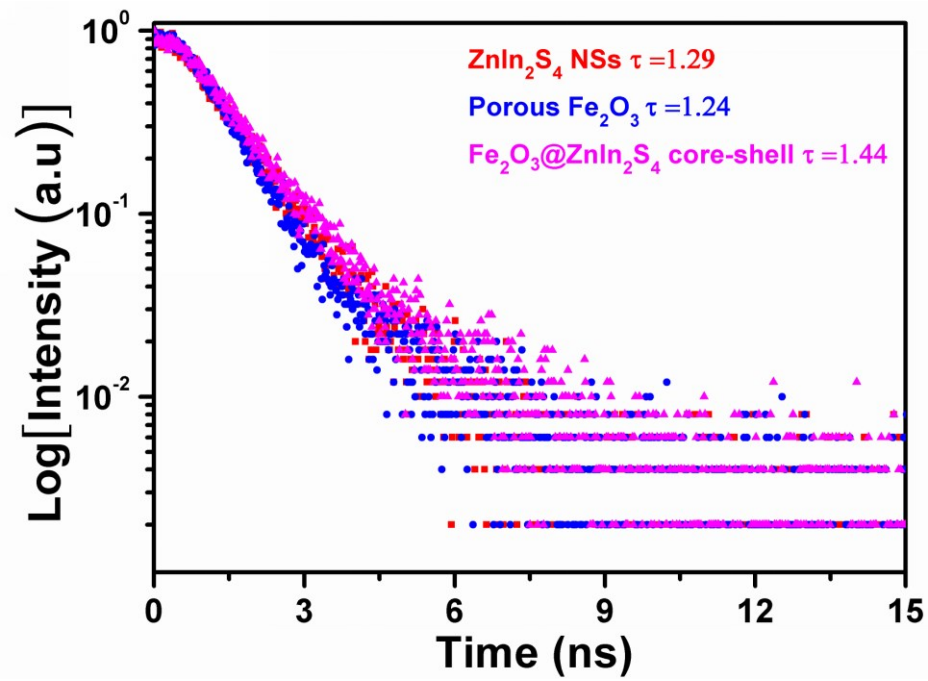

Figure S11. Time-resolved transient PL decay curves of Fe_2O_3, $ZnIn_2S_4$ and Fe_2O_3@$ZnIn_2S_4$ core-shell samples.

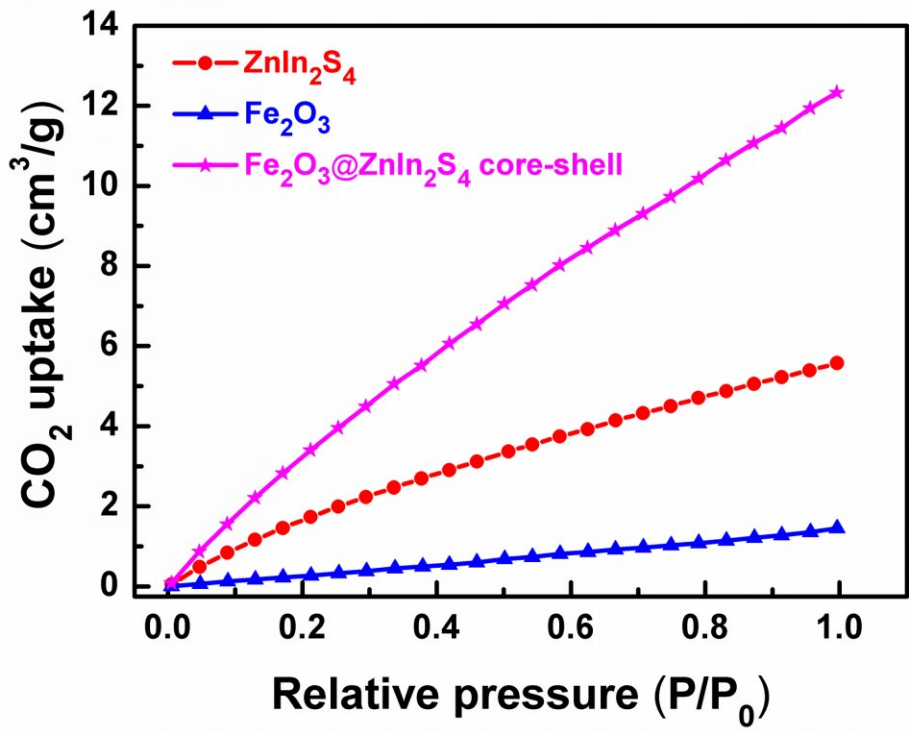

Figure S12. CO_2 adsorption capacity of Fe_2O_3, $ZnIn_2S_4$ and Fe_2O_3@$ZnIn_2S_4$ core-shell samples.

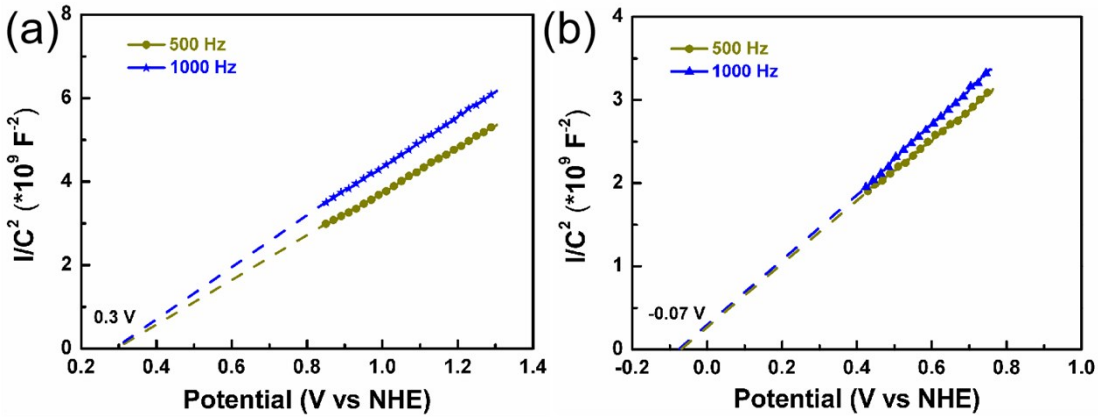

Figure S13. Mott-Schottky plots of (a) Fe_2O_3 and (b) $ZnIn_2S_4$.

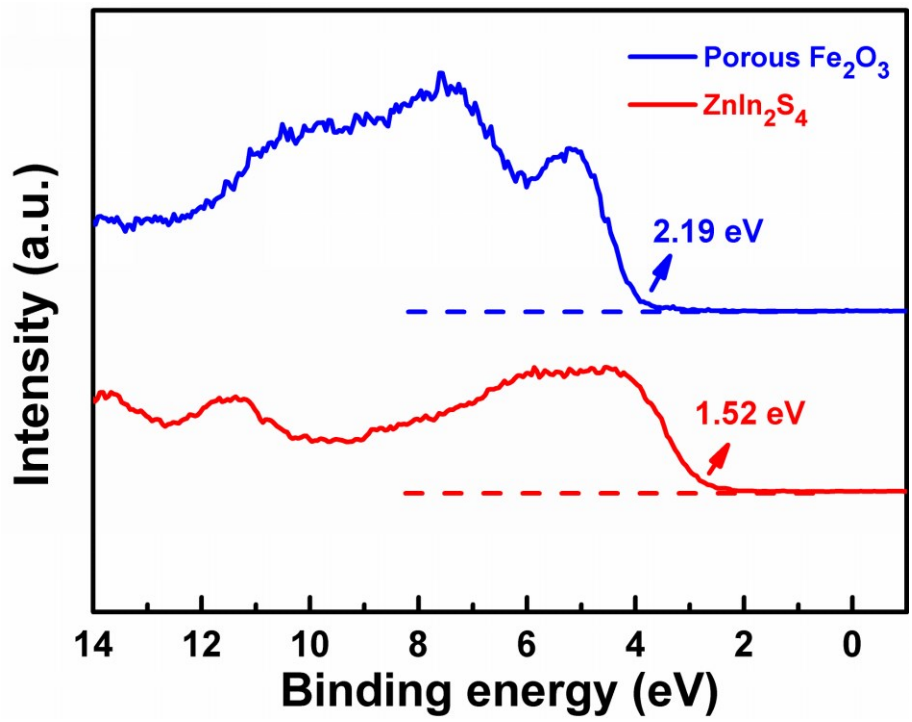

Figure S14. Valance band XPS spectra of Fe_2O_3 and $ZnIn_2S_4$.

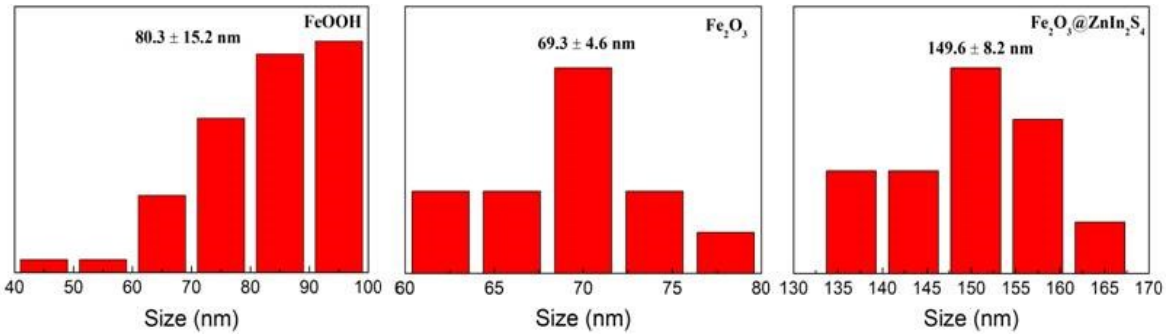

Chemical compound	**size distribution**
FeOOH NPs	80.3±15.2 nm
Fe_2O_3 NPs	69.3±4.6 nm
Fe_2O_3-$ZnIn_2S_4$ core-shell NPs	149.6±8.2 nm

Table S1. Size distribution of the FeOOH NPs, Fe_2O_3 NPs and Fe_2O_3-$ZnIn_2S_4$ core-shell NPs.

Catalysts	Products	Activity (CO) /μmol g^{-1} h^{-1}	reference
Fe_2O_3@$ZnIn_2S_4$	CO	**37.13**	This work
$SnFe_2O_4$/α-Fe_2O_3	CO	2.87	1
g-C_3N_4/Bi_2O_2[BO_2(OH)]	CO	6.09	2
ZnO/$ZnWO_4$/g-C_3N_4	CO	13.19	3
$SnFe_2O_4$-CN	CO	7.56	4
20 wt%Bi_2S_3 QDs / g-C_3N_4	CO	16.74	5
CdS/BiOI	CO	3.32	6
40 wt%Bi_2O_3/g-C_3N_4	CO	5.92	7
CdS/$CdWO_4$	CO	1.47	8

Table S2. Compare the recently reported photocatalytic activity of Z-Scheme materials in CO_2.

Reference:

[1] Jia Y, Zhang W, Do J Y, et al. Z-Scheme $SnFe_2O_4$/α-Fe_2O_3 Micro-octahedron with Intimated Interface for Photocatalytic CO_2 Reduction. Chemical Engineering Journal, (402) 2020 126193.

[2] Guo L, You Y, Huang H, et al. Z-scheme g-C_3N_4/$Bi_2O_2[BO_2(OH)]$ heterojunction for enhanced photocatalytic CO_2 reduction. Journal of Colloid and Interface ence, (568) 2020 139-147.

[3] Zhu L, Li H, Xu Q, et al. High-efficient separation of photoinduced carriers on double Z-scheme heterojunction for superior photocatalytic CO_2 reduction. Journal of Colloid and Interface ence, (564) 2019 303-312.

[4] A Y J, A H M, B W Z, et al. Z-scheme $SnFe_2O_4$-graphitic carbon nitride: Reusable, magnetic catalysts for enhanced photocatalytic CO_2 reduction. Chemical Engineering Journal, (383) 2020 123172.

[5] Guo R T, Liu X Y, Qin H, et al. Photocatalytic reduction of CO_2 into CO over nanostructure Bi_2S_3 quantum dots/g-C_3N_4 composites with Z-scheme mechanism. Applied Surface ence, (500) 2019 144059.

[6] Zhou R H, Wei Z H, Li Y Y, et al. Construction of visible light-responsive Z-scheme CdS/BiOI photocatalyst with enhanced photocatalytic CO_2 reduction activity. Journal of Materials Research, (34) 2019 3907-3917.

[7] Hao P, Guo R T, He L, et al. Synthesis of Bi_2O_3/g-C_3N_4 for enhanced photocatalytic CO_2 reduction with a Z-scheme mechanism. RSC Advances, (64) 2019 37162-37170.

[8] Li Y Y, Wei Z H, Fan J B, et al. Photocatalytic CO_2 reduction activity of Z-scheme CdS/$CdWO_4$ catalysts constructed by surface charge directed selective deposition of CdS. Applied Surface Science, (483) 2019 442-452.